www.czasopisma.pan.pl PAN POLSKA AKADEMIA NAUK www.journals.pan.pl

Arch. Metall. Mater. **64** (2019), 1, 103-112

DOI: 10.24425/amm.2019.126224

A. JĘDRZEJEWSKA*#, D. SIBERA*, R. PEŁECH**, R. JĘDRZEJEWSKI***, U. NARKIEWICZ*

NANOCOMPOSITES GRAPHENE/$CoFe_2O_4$ AND GRAPHENE/$NiFe_2O_4$ – PREPARATION AND CHARACTERIZATION

A series of nanocomposite graphene/$CoFe_2O_4$ and graphene/$NiFe_2O_4$ hybrid materials was synthesized via facile, one-pot solvothermal route. The materials were obtained using two pressure methods: synthesis in the autoclave and synthesis in the microwave solvothermal reactor. The use of a microwave reactor enabled to significantly shorten the synthesis time up to 15 min. All the syntheses were carried out in a solution of ethanol. The effect of processing conditions and composite composition on the physicochemical properties and electric conductivity was studied. The specific surface area, density, morphology, phase composition, thermal properties and electric conductivity of the obtained composites were investigated. The results of studies of composites obtained in an autoclave and in a microwave reactor were compared.

Keywords: Graphene, Nanocomposites, $CoFe_2O_4$, $NiFe_2O_4$

1. Introduction

Spinel ferrites (MFe_2O_4, M = metal cation) are very interesting materials because they are stable chemically and magnetically and have a small energy band gap [1,2]. The materials are used in analytical biochemistry, medicine, removal of heavy metals and biotechnology. They have been increasingly applied to immobilize proteins, enzymes, and other bioactive agents due to their unique advantages. Nano-$CoFe_2O_4$ spinel is a hard magnetic material with a high coercivity, high cubic magneto crystalline anisotropy, excellent chemical stability and mechanical hardness. Nickel ferrite ($NiFe_2O_4$) has been also intensively investigated as one of the magnetic nanomaterials. Nickel ferrite has an inverse spinel structure. Nickel ferrite shows super-paramagnetic behaviour and it has various applications.

The possessed properties make the ferrites ideal candidates in catalytic/photo catalytic applications, electro chemical energy storage devices, gas/humidity sensors, microwave devises, magnetic resonance imaging, magnetic fluids, spintronics, solar cells, high density recording media and power transformer in electric and telecommunication applications [3-9]. Large-scale applications of ferrites with small particles and tailoring of specific properties have prompted the development of widely used chemical methods, including combustion, coprecipitation, sol-gel, mechanical alloying and precipitation or microwave solvothermal process for the fabrication of stoichiometric and chemically pure spinel ferrite nanoparticles [10-13].

Graphene has recently become a new promising candidate as the support for metals because of its excellent properties. Graphene is an ideal material for electrochemistry because it exhibits improved features, such as very large 2-D electrical conductivity, very fast heterogeneous electron transfer, large surface area and low cost [14,15].

In the literature many methods have been described for preparing nanocomposites of graphene / XFe_2O_4 where X is – Co, Mn, Zn, Ni, etc. The most commonly used methods are preparation in autoclave and annealing processes [16-20]. In this work, we demonstrate the synthesis of graphene/$NiFe_2O_4$ and graphene/$CoFe_2O_4$ nanohybrid composites using a solvothermal strategy in a microwave reactor and in an autoclave. The syntheses were carried out in a solution of ethanol. We investigated the effect of synthesis parameters on the quality of the obtained nanocomposites. The specific surface area, density, morphology, phase composition, thermal properties and electric conductivity of the obtained composites were investigated.

2. Experimental

Graphene/$CoFe_2O_4$ and grapheme/$NiFe_2O_4$ hybrid materials were synthesized by applying a microwave solvothermal reactor (ERTEC Magnum II) and an autoclave (Berghof). The procedure for the preparation of composites has already been described in our previous work [21]. Graphene Nanopowder

* WEST POMERANIAN UNIVERSITY OF TECHNOLOGY, FACULTY OF CHEMICAL TECHNOLOGY AND ENGINEERING, INSTITUTE OF CHEMICAL AND ENVIRONMENT ENGINEERING, 10 PUŁASKIEGO STR., 70-322 SZCZECIN, POLAND
** WEST POMERANIAN UNIVERSITY OF TECHNOLOGY, FACULTY OF CHEMICAL TECHNOLOGY AND ENGINEERING, INSTITUTE OF ORGANIC CHEMICAL TECHNOLOGY, 10 PUŁASKIEGO STR., 70-322 SZCZECIN, POLAND
*** WEST POMERANIAN UNIVERSITY OF TECHNOLOGY, FACULTY OF MECHANICAL ENGINEERING AND MECHATRONICS, INSTITUTE OF MATERIALS SCIENCE AND ENGINEERING, 19 PIASTÓW AV., 70-322 SZCZECIN, POLAND
# Corresponding author: Anna.Jedrzejewska@zut.edu.pl

AO-3 was used for the synthesis. In the first preparation step a mixture of graphene in ethanol (sonification for 20 minutes) was prepared. In next step cobalt or nickel nitrate and iron nitrate were added to this solution and stirred. The amount of cobalt, nickel and iron nitrates corresponded to a content of 5 wt.% or 25 wt.% $CoFe_2O_4$ or $NiFe_2O_4$ spinel in the composite. Ammonia water was used for the precipitation of the corresponding hydroxides (cobalt, nickel and iron hydroxide). Ammonia water was added until pH = 12 was reached. Then, the obtained solution was subjected to a pressure treatment. The temperature applied in the process conducted in the autoclave was 120°C, 160°C or 200°C. The synthesis time was 12 h at each temperature. Pressure treatment in the microwave solvothermal reactor was much shorter, the solution was treated here for 15, 30 or 45 min, under a pressure of 4 to 5 MPa. The synthesis time in the microwave reactor was measured from the moment when the predetermined pressure was reached. In the last step the obtained materials were filtered and washed with deionised water to remove salt residues. Finally, the materials were dried at 80°C for 24 h.

The structure and crystallinity was determined by powder X-ray diffraction studies using a PANalytical Empyrean X-ray diffractometer. Cu-Kα radiation with wavelength $\lambda = 1.54$ Å was used for the study. The obtained XRD pattern was analyzed in the X'Pert High Score Plus program using the ICDD PDF-4+ database.

Microstructure and morphology of obtained samples were characterised by TEM technique (FEI TECNAI G2 F-20 S TWIN).

The specific surface area of the obtained samples was determined by physical adsorption of N_2 at –196°C using Quantachrome Quadrasorb Instruments. Density measurements were made on the Micro-Ultrapyc 1200e.

The thermal properties of nanocomposites were determined by thermogravimetric analysis using DTA-Q600 SDT TA Instruments thermal imaging.

Electrical properties were determined by measuring the resistivity of the layer containing the test material dispersed in paraffin. Samples were prepared by adding different amounts of the test powder to 1 g of the molten paraffin. The suspension of powder in paraffin was placed in an ultrasonic bath, and the ultrasound power was adjusted to solidify the sample in the molds of copper.

3. Results and discussion

The structure and crystallinity was determined by powder X-ray diffraction studies.

As shown in Fig. 1 and Fig. 2, peaks shown on the nanocomposite pattern can be ascribed to the rhombohedral phase of $CoFe_2O_4$ structure (ICDD 00-003-0864) with small crystallites. The peaks shown in Fig. 3 and Fig. 4 can be ascribed to the rhombohedral phase of $NiFe_2O_4$ structure (ICDD 01-074-2081). In all the composites (Fig. 1-4) the graphite phase with a characteristic peak at 2Theta = 26.52°, indicating an interlayer spacing of 0.336 nm with an index of (002) can be ascribed. Some small peaks of carbon (ICDD 00-026-1076) can be identified as well. Stacking peak of graphene sheets could indicate the agglomeration occurring in the hybrid material and formation of graphite-like structure.

The analysis of XRD patterns made for samples prepared in microwave reactor (40 atm, 15-45 min) as well as in autoclave (12 h, 120-200°C) showed that all composites had the same phase composition. Using XRD analysis, it was confirmed that $NiFe_2O_4$ and $CoFe_2O_4$ were obtained in all composites. The synthesis conditions had no significant effect on the phase composition of the obtained samples. Also, the method of the preparation of samples did not affect the phase composition of the obtained materials. It should be noted that the use of a microwave reactor during the preparation of composite materials significantly reduced

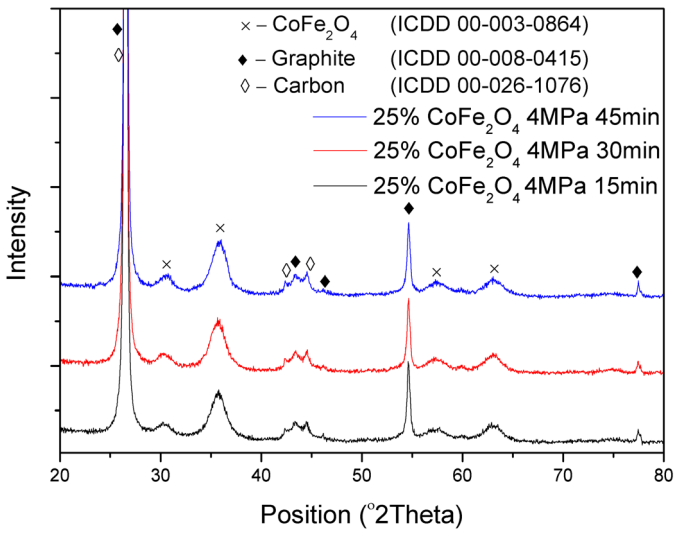

Fig. 1. Comparison of XRD spectra of graphene/25% $CoFe_2O_4$ composites obtained in a microwave reactor in ethanol at 4 MPa at various reaction time of 15-45 min

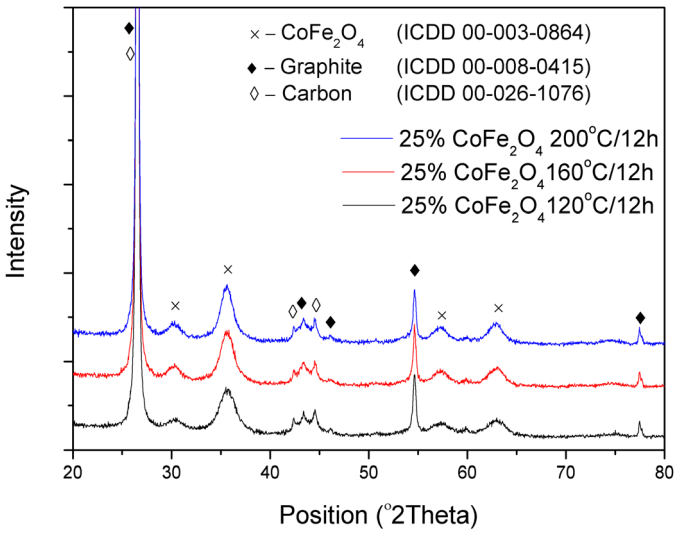

Fig. 2. Comparison of XRD spectra of graphene/25% $CoFe_2O_4$ composites obtained in a autoclave for reaction time of 12 h at various temperature in the range of 120-200°C

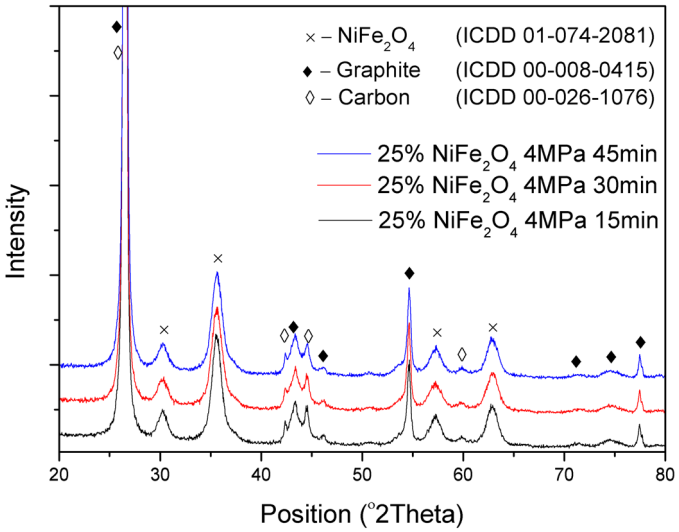

Fig. 3. Comparison of XRD spectra of graphene/25% $NiFe_2O_4$ composites obtained in a microwave reactor in ethanol at 4 MPa at various reaction times of 15-45 min

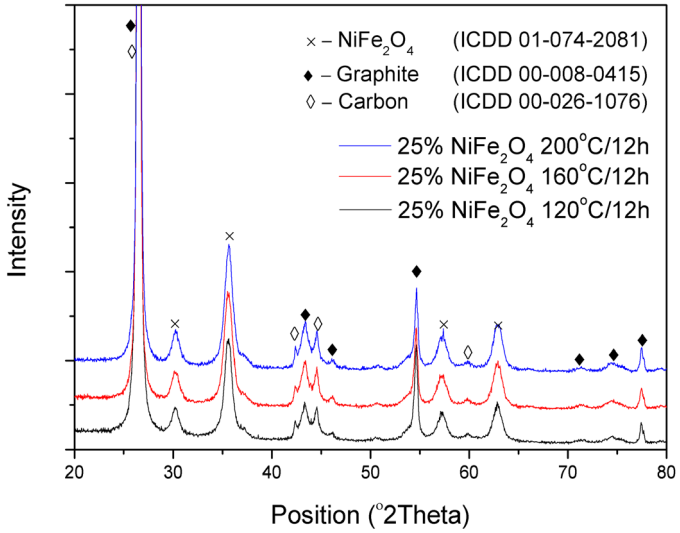

Fig. 4. Comparison of XRD spectra of graphene/25% $NiFe_2O_4$ composites obtained in a autoclave for reaction time of 12 h and at various temperature in the range of 120-200°C

the synthesis time. The average crystallite size of $CoFe_2O_4$ in all composites was estimated by the Scherrer formula to 5.0 nm and the lattice parameter was 8,35 Å. The average crystallite size of $NiFe_2O_4$ in all composites was estimated to 7.0 nm and the lattice parameter was 8,35 Å. The calculations showed that the synthesis parameters did not affect the crystallite size in the obtained composites.

Microstructure and morphology of selected obtained products were characterised by TEM technique. The morphology of various graphene/$CoFe_2O_4$ andgraphene/$NiFe_2O_4$ samples obtained in the microwave solvothermal reactor and in the autoclave TEM is presented in the images in Fig. 5 and 6. All the samples G/$NiFe_2O_4$ and G/$CoFe_2O_4$ exhibited a typically wrinkled, sheet-like structure. In the G/$CoFe_2O_4$ composites obtained in the microwave reactor, the crystallite size slightly increased with the elongation of the synthesis time. Increasing of the synthesis time also affected the agglomeration in these composites. The increase of pressure did not affect the size of crystallites in these samples. In G/$NiFe_2O_4$ samples obtained in the microwave reactor, crystallite size were similar in all the composites. In these materials, the length of the synthesis time and increase of the pressure did not affect the size of crystallites (Fig. 6). The opposite situation was observed in the case of G/$NiFe_2O_4$ composites obtained in autoclave. In these samples the $NiFe_2O_4$ crystallinity was higher than in the samples obtained in the reactor. Furthermore, the temperature affected the size of crystallites and the agglomeration of $NiFe_2O_4$ crystallites. However, the results obtained from the XRD analysis showed that the synthesis conditions did not affect the size of the crystallites. This may suggest that in TEM images single crystallite aggregates can be observed. In addition, $CoFe_2O_4$ and $NiFe_2O_4$ crystallites were distributed homogeneously on the surface of graphene. In some places they formed small clusters in which single crystallites agglomerated. The obtained results showed that the layer of graphene did not allow for an increase of dopant crystallites dopant, whatever even the various synthesis conditions. A similar relationship was observed by Heidari et al. on composites obtained from exfoliated graphite [22].

The structural properties of the obtained materials were characterized by the determination of the specific surface area and density. The theoretical density of the pure bulk $CoFe_2O_4$ and pure bulk $NiFe_2O_4$ is 5,30 g/cm^3 [23] and 5,39 g/cm^3 [24], respectively. Since the density of pure spinels is higher than the density of pure graphene, it was expected that the density of composites would also be higher than the density of graphene. If the content of spinels in the composites would be at the same percentage level, no differences in density measurements were expected. With a decreasing content of the admixtures the density of the composites should also decrease.

The results of the density measurements are shown in Tables 1 and 2. All obtained materials had a higher density than pure graphene, then the obtained results confirmed that the spinel $CoFe_2O_4$ or spinel $NiFe_2O_4$ was present in the samples. In addition, no significant differences were observed depending on the type of dopant and on the application of the preparation method. The obtained results also showed that the parameters of the composite preparation process did not affect the results of density. The density depended only on the content of the admixture in the composite. The composites with an admixture content of 5 wt.% had the density of about 0.3 g/cm^3 lower than the composites with a content of 25 wt.% admixture.

The specific surface area of the composites were measured by physical adsorption of N_2 at –196 °C using a Quadrasorb apparatus. Specific surface area was determined by the multipoint BET (Brunauer-Emmet-Teller equation) [25] method with the N_2 adsorption isotherm over a relative pressure (P/P_0) in the range of 0.05-0.20. The total pore volume, V_p, including both micropores and mesopores, was estimated by converting the amount of N_2 gas adsorbed at a relative pressure of 0.99 to liquid

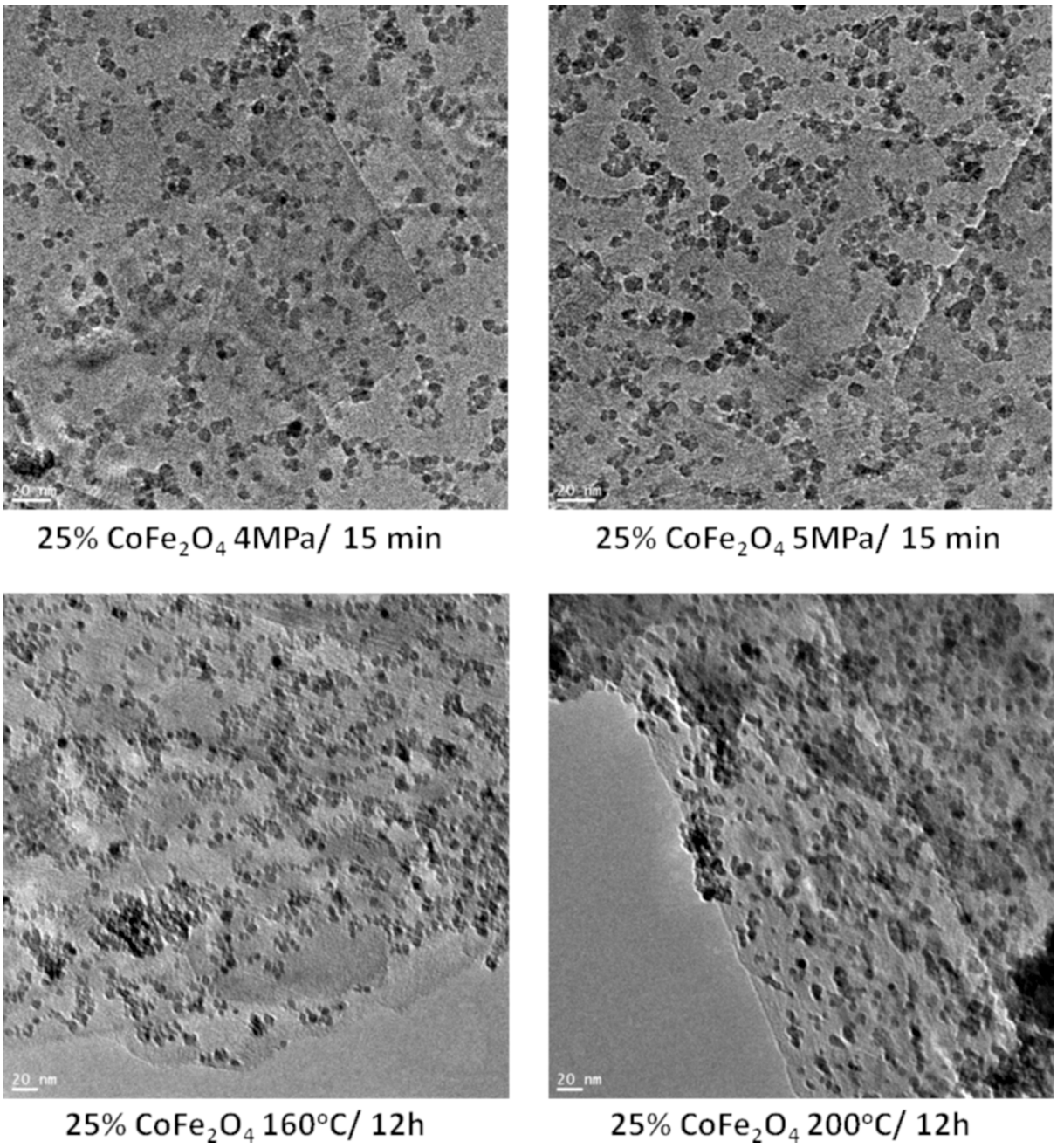

Fig. 5. TEM pictures of graphene/25% $CoFe_2O_4$ composites obtained in microwave reactor at 4 MPa and 5 MPa and in autoclave at 160°C and 200°C

volume of the adsorbate (N_2). Micropore volumes (<2 nm), V_{mic}, was determined using the Density Functional Theory (DFT).

According to the studies of the specific surface, the composite containing $CoFe_2O_4$ had higher surface areas than pure graphene. This is probably due to the small size of the spinel crystallites that formed in the composites. According to Fig. 5 showing the crystallites of the G/$CoFe_2O_4$ composites obtained in a microwave reactor were smaller and had a lower tendency to agglomerate. In the case of these composites, it can be observed that the increase in the synthesis pressure and the extension of the synthesis time had a slight influence on the structural properties of the produced materials. However, in the case of composites obtained in the autoclave, the specific surface area was similar to that of puregraphene (Table 1 and 2). In these composites, we observed $CoFe_2O_4$ crystallites of larger size and greater tendency to agglomerate, which affected the value of the specific surface area. Graphene/$NiFe_2O_4$ composites had a smaller specific surface area than pure graphene (composites produced in the autoclave) or similar to that of graphene in the case of the composites obtained in the reactor. The $NiFe_2O_4$ crystallites observed in TEM images had larger mean crystallite size than that of $CoFe_2O_4$ crystallites.

The addition of both spinels to graphene had an effect on the microporosity of the obtained composites. All materials had a lower content of micropores than pure graphene, which may indicate that the nanocrystals of $CoFe_2O_4$ and $NiFe_2O_4$ could be partially deposited in the pores of the carbonaceous material, clogging them.

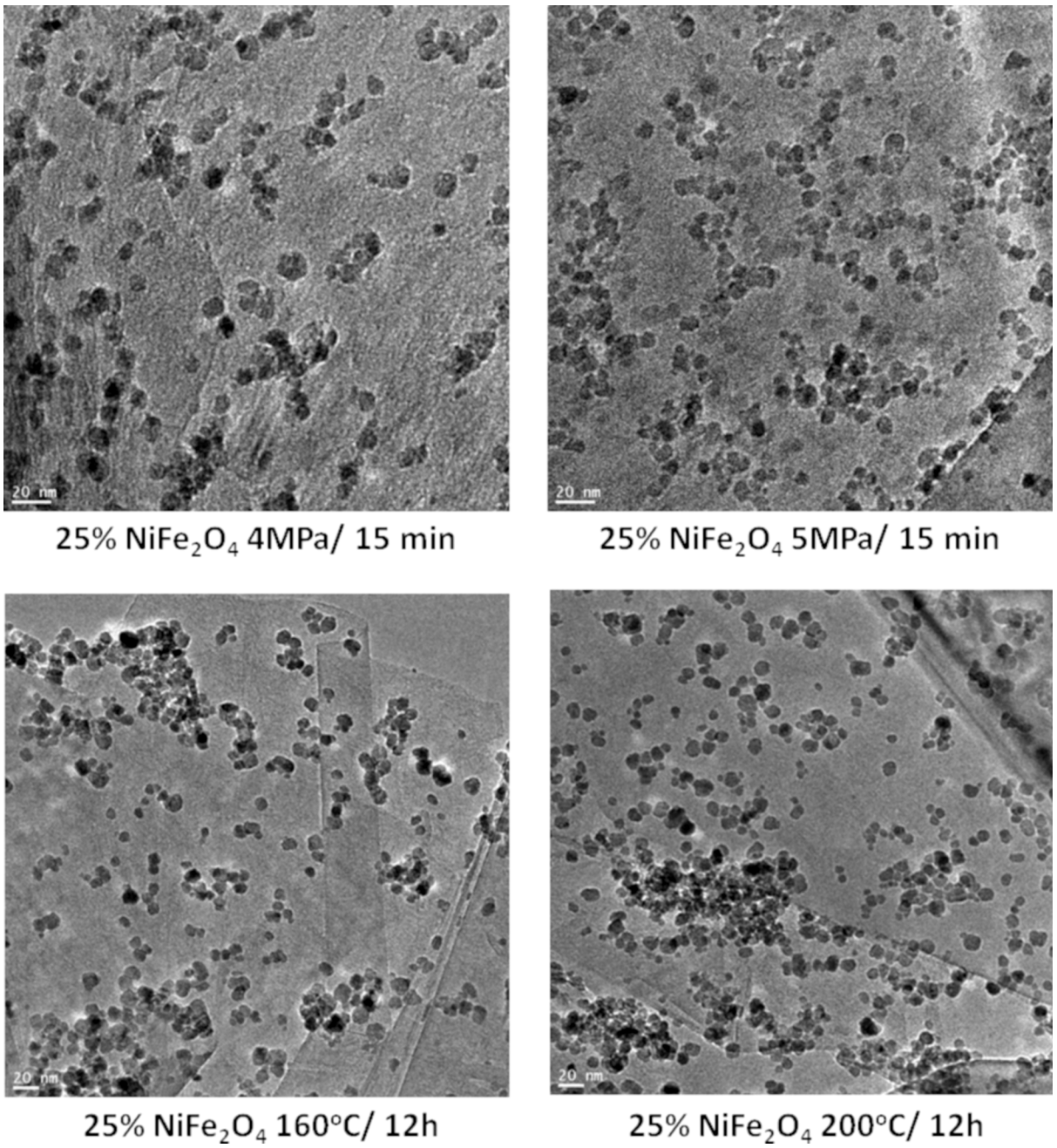

Fig. 6. TEM pictures of graphene/25% $NiFe_2O_4$ composites obtained in microwave reactor at 4 MPa and 5 MPa and in autoclave at 160°C and 200°C

TABLE 1

Samples obtained in microwave solvothermal reactor

Name of samples	Specific surface area [m^2/g]	Total Pore Volume [cm^3/g]	Micropore Volume [cm^3/g]	Density [g/cm^3]	Crystallite size [nm]
Graphene	64	0.109	0.020	1.78	—
5% $CoFe_2O_4$ 4 MPa/15 min	48	0.138	0.013	2.09	4.5
25% $CoFe_2O_4$ 4 MPa/15-45 min	70-77	0.134-0.157	0.016-0.017	2.37-2.42	5.5
25% $CoFe_2O_4$ 4,5 MPa/15-45 min	72-73	0.137-0.148	0.015-0.016	2.38-2.41	5.0
25% $CoFe_2O_4$ 5 MPa/15-45 min	73	0. 116-0.147	0.016-0.018	2.42-2.44	5.0
5% $NiFe_2O_4$ 4 MPa/15min	52	0.157	0.013	2.05	6.5
25% $NiFe_2O_4$ 4 MPa/15-45 min	63-64	0.123-0.129	0.015	2.31-2.36	7.0
25% $NiFe_2O_4$ 4,5 MPa/15-45 min	63-67	0.121-0.188	0.015-0.016	2.32-2.46	7.5
25% $NiFe_2O_4$ 5 MPa/15-45 min	64-66	0.124-0.135	0.015-0.016	2.33-2.46	7.0

TABLE 2

Samples obtained in autoclave

Name of samples	Specific surface area [m^2/g]	Total Pore Volume [cm^3/g]	Micropore Volume [cm^3/g]	Density [g/cm^3]	Crystallite size [nm]
Graphene	64	0.109	0.020	1.77	—
5% $CoFe_2O_4$ 120°C/12h	38	0.132	0.011	2.05	4.5
25% $CoFe_2O_4$ 120°C/12h	66	0.095	0.014	2.37	5.0
25% $CoFe_2O_4$ 160°C/12h	68	0.125	0.015	2.37	5.0
25% $CoFe_2O_4$ 200°C/12h	59	0.117	0.013	2.39	5.5
5% $NiFe_2O_4$ 120°C/12h	48	0.134	0.012	2.01	7.0
25% $NiFe_2O_4$ 120°C/12h	54	0.144	0.012	2.34	7.5
25% $NiFe_2O_4$ 160°C/12h	54	0.115	0.012	2.34	7.0
25% $NiFe_2O_4$ 200°C/12h	56	0.130	0.014	2.43	6.5

The thermal properties of nanocomposites were determined by thermogravimetric analysis. The results obtained for the selected samples are shown in Figures 7.

The tested materials exhibited thermal stability up to about 300°C. The weight loss below this temperature was due to the evaporation of water from the surface and from the pores of the materials. In all tested samples, the course of thermogravimetric curves is similar. The mass loss of the tested composites started above 350°C. It was due to the gasification of carbon and the removal of the resulting carbon oxides [26-28]. Many researchers observed thermal stability in their composites at a similar level [29-31]. Above 450°C the weight loss reached 8 %, which could result from detachment of oxygen bound to on the graphene surface. Carbon gasification process ended at 830°C. The total weight loss was about 74-78%, than the remaining materials were composed of $CoFe_2O_4$ or $NiFe_2O_4$ only. The weight loss

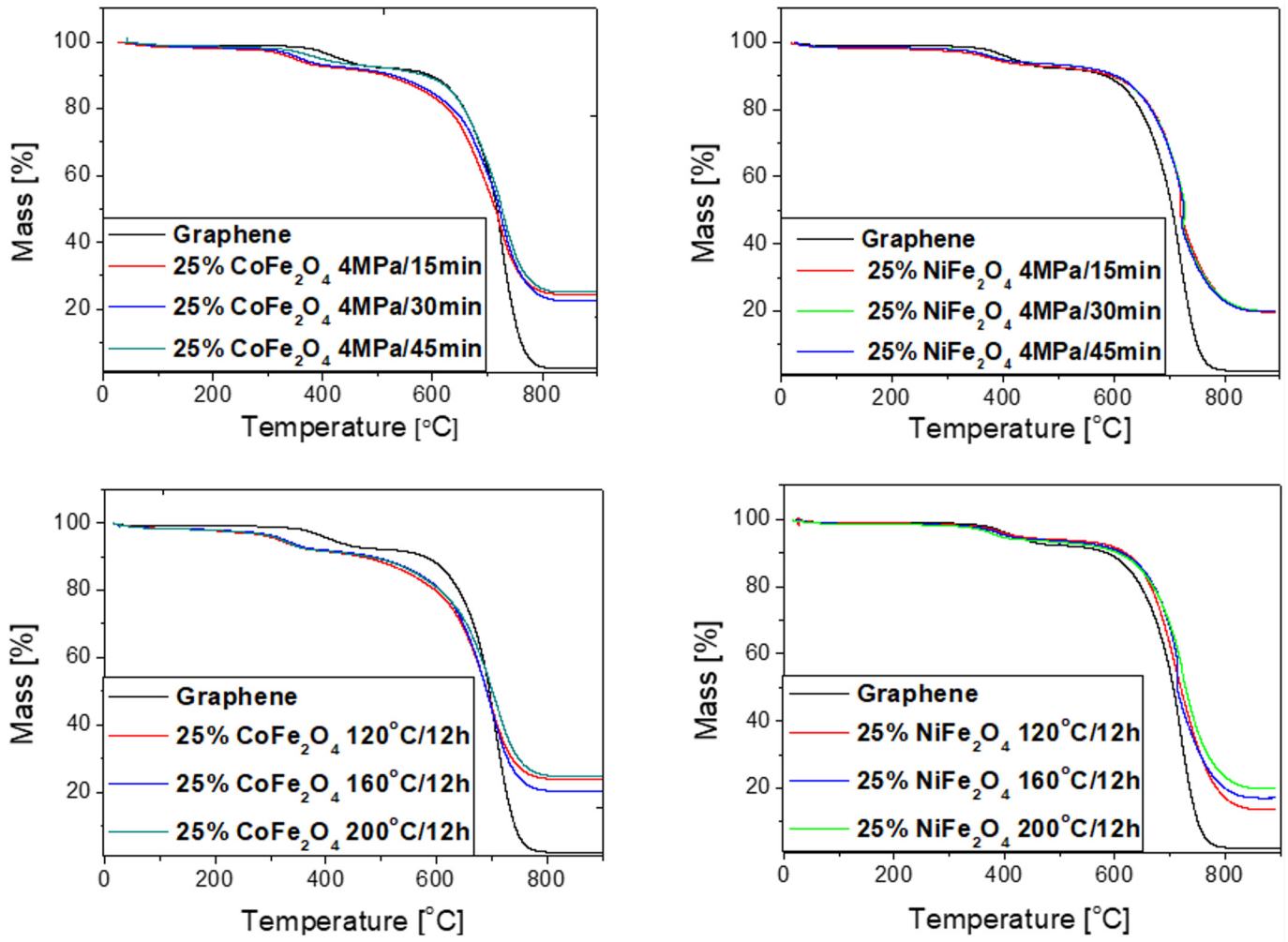

Fig. 7. TG curves of selected samples obtained in microwave reactor at 4 MPa and in autoclave at various reaction temperature: 120°C, 160°C and 200°C

in the range of 74-78% also confirmed the intended composition of the obtained composites – 75 wt.% of carbon and 25 wt.% of $CoFe_2O_4$ or $NiFe_2O_4$. The previously analysed XRD spectra also confirmed that the samples consisted only of carbon and $CoFe_2O_4$ or $NiFe_2O_4$. All obtained composites, regardless of the kind of admixture, had lower thermal stability than pure graphene. It should be noted that composites with $NiFe_2O_4$ had greater thermal stability than graphene/$CoFe_2O_4$ composites. However, when the temperature exceeded 700°C in the case of composites with $CoFe_2O_4$ and about 450°C for samples with $NiFe_2O_4$, an improvement of thermal stability in relation to pure graphene was observed (Fig. 8). An increase of pressure, temperature and synthesis time did not improve the thermal stability of the obtained samples. In Fig. 8 the results of the TG for the different samples to a temperature of 600°C are presented. Yao et al. in their work observed decarbonisation of graphene at lower temperatures at about 382°C [32]. Xiao et al. in their studies also observed decarbonisation of graphene in composites at lower temperatures [18]. In our composites a decarbonisation of the carbon skeleton we observed only above 600°C, then we obtained very stable composites.

Electrical properties were determined by measuring the resistivity of the layer containing the test material dispersed in paraffin. A schematic diagram of the system applied to carry out the conductivity measurements is shown below.

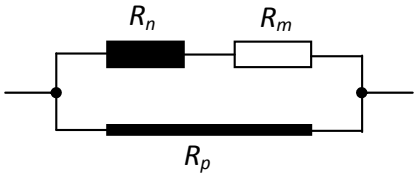

Where: R_n – resistance of the nanocomposite, R_m – resistance of the matrix, R_p – resistance of the percolation paths.

$$R_n = \rho_n \cdot C_n \cdot l$$

$$R_m = \rho_m \cdot (1 - C_n) \cdot l$$

Where: C_n – concentration of the nanocomposite, ρ_n, ρ_m – resistivity of nanocomposite and matrix(paraffin).Then the conductivity of the system can be described as

$$G = \frac{1}{C_n(\rho_n - \rho_m) + \rho_m} + G_k \cdot N$$

Where: G_k – conductivity of the percolation path, N – the number of percolation paths.

For the classic percolation network, the conductivity of the entire system changes as a result of the rapid disappearance of electrical continuity in the percolation threshold. For $C < C_p$,

$$G = \frac{1}{C_n(\rho_1 - \rho_2) + \rho_2}$$

while for $C_n > C_p$, because $\rho_n \gg \rho_m$ to

$$G_K \cdot N >> \frac{1}{C_n(\rho_n - \rho_m) + \rho_m}$$

then we can assume:

$$G = G_k \cdot N$$

Then taking

$$N\alpha(C_n - C_p)^n$$

Where: C_p – percolation threshold value, n – critical exponent characterizing the increase in the probability of creating percolation paths, G_k – characterizes the conductivity of the emerging paths.

Finally, we obtain:

$$G = G_0 \cdot (C_n - C_p)^n \qquad \text{X}$$

Where G_0 – conductivity of the nanocomposite.

The figures below shows a percolation curve of conductivity against concentration of the nanocomposite along with the parameters of the equation X.

The percolation region for pure graphene samples was in the range of the mass fraction of pure graphene in the wax of 0.025-0.04. In the case of composites containing 5 wt% of spinel $NiFe_2O_4$ or $CoFe_2O_4$ the percolation region moved and was in the

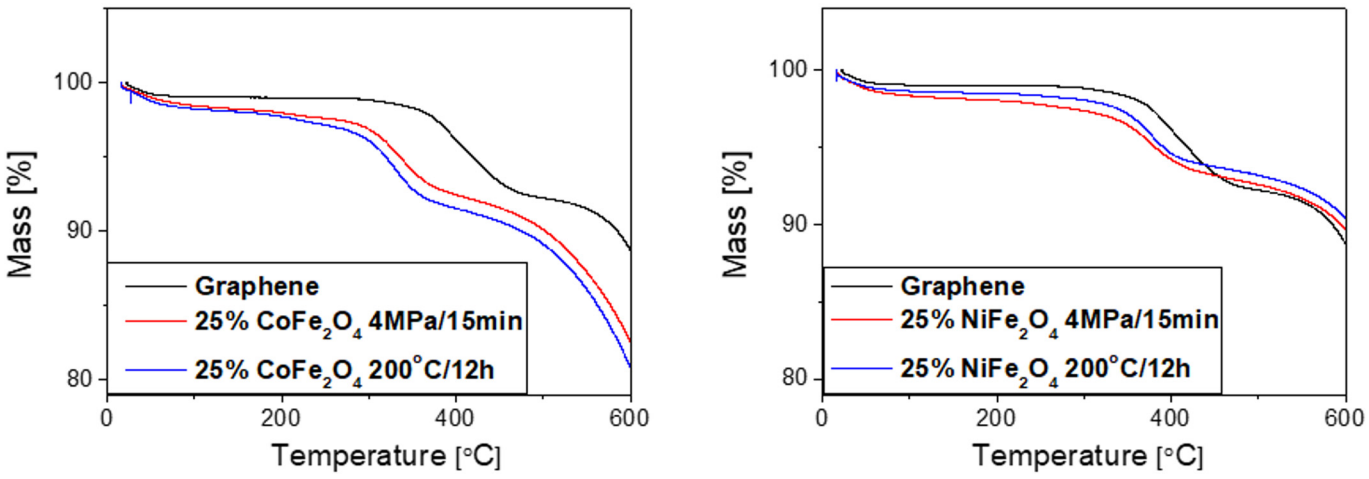

Fig. 8. TG curves of selected samples obtained in microwave reactor at 4 MPa and in autoclave at 200°C

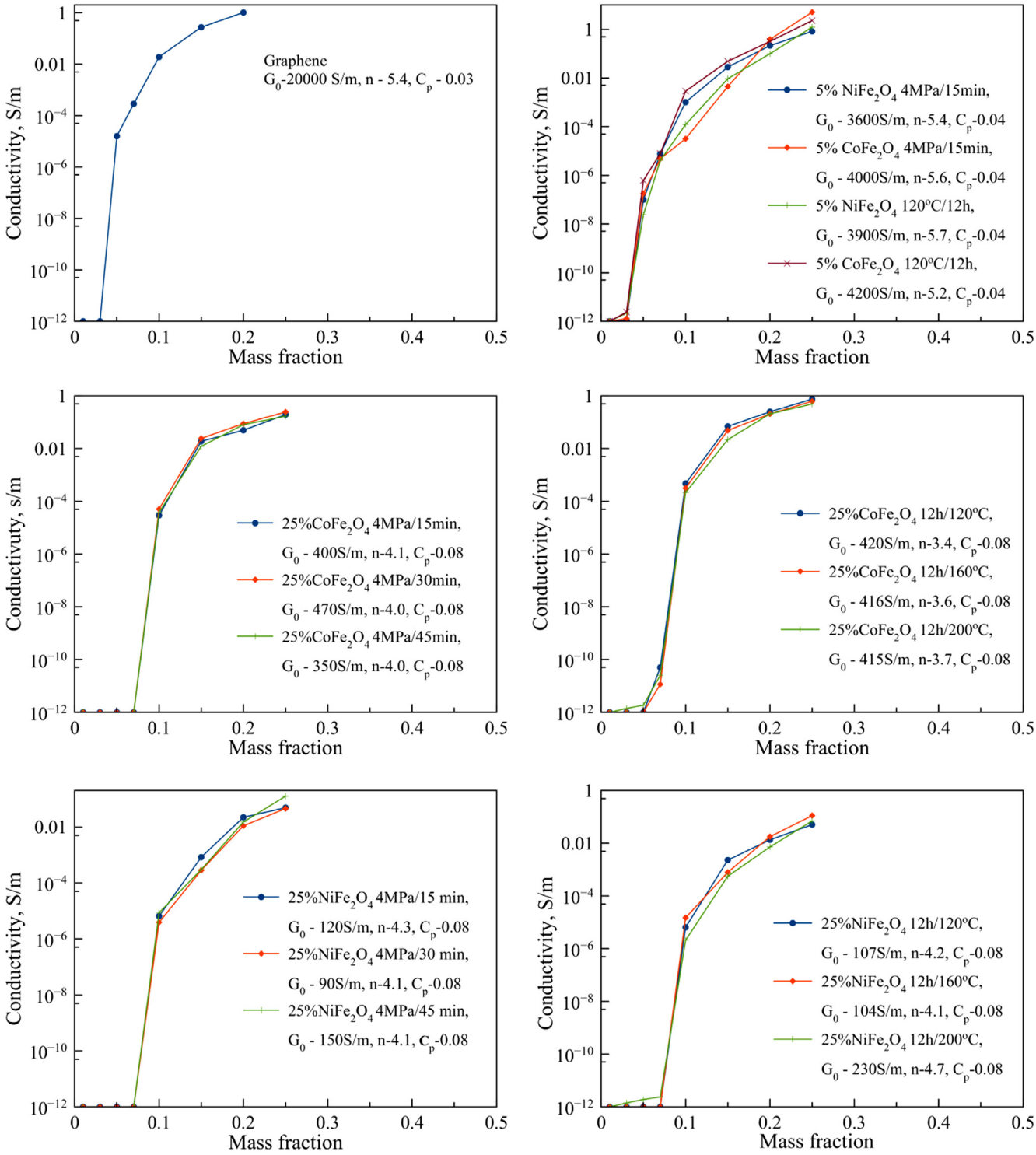

Fig. 9. Percolation curves of electrical conductivity as a function of nanocomposite concentration

range of 0.03-0.05. However, for composites containing 25wt.% of $CoFe_2O_4$ or $NiFe_2O_4$ spinel, the percolation region was in the range of 0.07-0.09. Then, an increase of the spinel content in the nanocomposite caused an increase of the percolation threshold. This was a result of a more difficult creation of graphene percolation pathways. The conductivity of the spinel particles was at the level of matrix conductivity (wax) [33,34], forming insulation bridges between the graphene platelets. Schematic creation of bridges is shown in the Fig. 10.

The value of the critical exponent n varied depending on the way the synthesis was conducted as well as on the type of spinel applied. This may indicate different mechanisms of percolation path formation. It can be a result of, for example, differences in grain sizes of the synthesized spinel and the tendency of spinel particles to agglomerate on the surface of graphene sheets. Based on the G_0 parameter, it can be concluded that the addition of spinel significantly affected the conductivity of the nanocomposite by lowering it. The method of preparation of the composite did

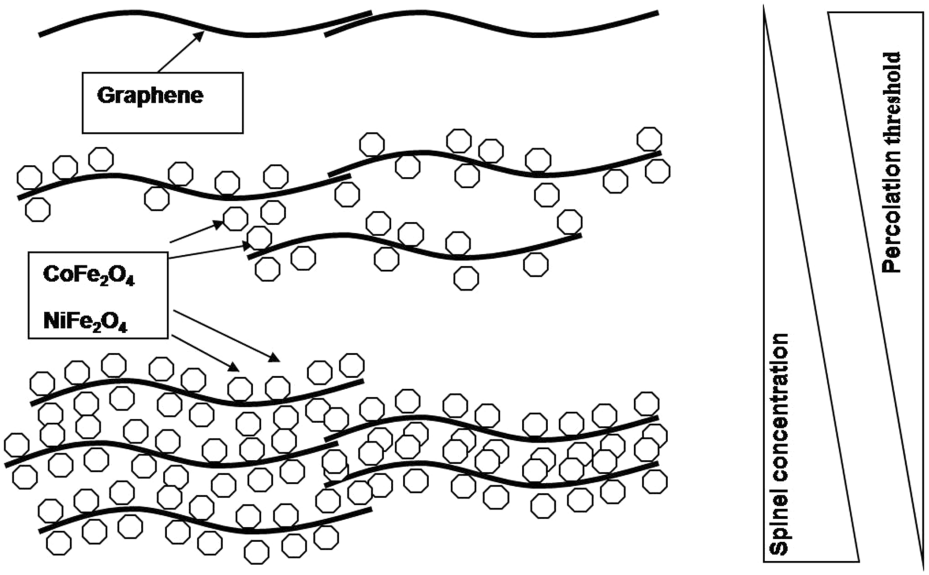

Fig. 10. Schematic representation of the creation of insulation bridges

not significantly affect the G_0 parameter. It was significantly influenced by the type of spinel introduced into the composite. G_0 for composites with 25 wt.% of $NiFe_2O_4$ was in the range of 90-230 S/m and for $CoFe_2O_4$ – in the range of 350-470 S/m. For composites containing 5 wt.% of $NiFe_2O_4$ it was in the range of 3600-3900 S/m and for $CoFe_2O_4$ 4000-4200 S/m. This effect is probably due to a larger particle size of $NiFe_2O_4$ (average size of 7 nm) than that of $CoFe_2O_4$ (5 nm). In addition, according to the TEM images the spinel $NiFe_2O_4$ easily agglomerated. This effect can additionally influence on the increase of distance between graphene layers, causing a decrease in conductivity.The conductivity of a nanocomposite in a non-pressed form should be understood here, that is, the density corresponding to the bulk density of the nanocomposite powder. This behavior showed the effective formation of the graphene-spinel nanocomposite.

4. Conclusions

The nanocomposites G/$CoFe_2O_4$ and G/$NiFe_2O_4$ were obtained in the microwave assisted solvothermal reactor or in the autoclave. The materials obtained in the microwave reactor were qualitatively comparable with identical materials obtained in the autoclave. The use of a microwave reactor shortened the preparation time to several minutes, when the synthesis time in the autoclave was calculated in hours. The synthesis parameters did not affect the structural properties. A kind of equipment (autoclave or microwave reactor) had a small effect on structural properties of the obtained materials. The content of admixtures had the greatest influence on the properties of the produced composites, especially in the case of electrical properties. Samples with 5 wt.% of spinel had better electrical properties than samples with 25 wt.% of admixture. The synthesis method and conditions may have a small influence on the formation of spinel aggregates on the surface of graphene, which can also affect the electrical properties.

Acknowledgments

This work was supported by project: LIDER/496/L-6/14/NCBR/2015 financed by The National Centre for Research and Development.
This work was presented during Inter Nano Poland 2018.

REFERENCES

[1] L. Cui, P. Guo, G. Zhang, Q. Li, R. Wang, M. Zhou, L. Ran, X.S. Zhao, Colloids and Interfaces A: Physicochem. Eng. Aspects. (2013), DOI: 10.1016/j.colsurfa.2013.01.064

[2] Z. Zi, Y. Sun, Z. Yang, J. Dai, W. Song, J. Magn. Magn. Mater. (2009), DOI: 10.1016/j.jmmm.2008.11.004

[3] G.A. El-Shobaky, A.M. Turky, N.Y. Mostafa, S.K. Mohamed, J. Alloy. Compd. (2010), DOI: 10.1016/j.jallcom.2009.12.115

[4] N.M. Deraz, J. Anal. Appl. Pyro. (2010), DOI: 10.1016/j.jaap.2010.03.002

[5] S. Rana, R.S. Srivastava, M.M. Sorensson, R.D.K. Misra, Mater. Sci. Eng. B (2005), DOI: 10.1016/j.mseb.2005.02.043

[6] Y. Fu, H. Chen, X. Sun, X. Wang, A. I. Ch. E. J. (2012), DOI: 10.1002/aic.13716

[7] A. Afkhami, H. Khoshsafar, H. Bagheri, T. Madrakian, Anal. Chim. Acta (2014), DOI: 10.1016/j.aca.2014.04.061

[8] E.K. Heidari, B. Zhang, M.H. Sohi, A. Ataie, J.-K. Kim, J. Mater. Chem. A (2014), DOI: 10.1039/C4TA00507D

[9] M.S. Khandekar, R.C. Kambale, J.Y. Patil, Y.D. Kolekar, S.S. Suryavanshi, J. Alloy. Comp. (2011), DOI: 10.1016/j.jallcom.2010.10.073

[10] K. Maaz, A. Mumtaz, S. K. Hasanain, A. Ceylan, J. Magn. Magn. Mater. (2007), DOI: 10.1016/j.jmmm.2006.06.003

[11] M. Houshiar, F. Zebhi, Z.J. Razi, A. Alidoust, Z. Askari, J. Magn. Magn. Mater. (2014), DOI: 10.1016/j.jmmm.2014.06.059

[12] S. Thakur, R. Rai, S. Sharma, Mater. Lett. (2015), DOI: 10.1016/j.matlet.2014.10.014

[13] P. Sivakumar, R. Ramesh, A. Ramanand, S. Ponnusamy, C. Muthamizhchelvan, Appl. Surf. Sci. (2012), DOI: 10.1016/j.apsusc.2012.03.099

[14] S. Kochmann, T. Hirsch, O.S. Wolfbeis, Trends Anal. Chem. (2012), DOI: 10.1016/j.trac.2012.06.004

[15] M. Wang, Y. Wang, H. Dou, G. Wei, X. Wang, Ceram. Int. (2016), DOI: 10.1016/j.ceramint.2016.03.085

[16] N. Li, M. Zheng, X. Chang, G. Ji, H. Lu, L. Xue, L. Pan, J. Cao, J. Sol. State Chem. (2011), DOI:10.1016/j.jssc.2011.01.014

[17] M.E. Uddin, N.H. Kim, T. Kuila, S.H. Lee, D. Hui, J.H. Lee, Comp. Part B (2015) DOI: 10.1016/j.compositesb.2015.05.029

[18] Y. Xiao, X. Li, J. Zai, K. Wang, Y. Gong, B. Li, Q. Han, X. Qian, Nano-Micro Lett. (2014) DOI:

[19] J. Huang, W. Wang, X. Lin, C. Gu, J. Liu, J. Power Sour. (2018), DOI: 10.1016/j.jpowsour.2018.01.029

[20] A. Mishra, V.K. Singh, T. Mohanty, J. Mater. Sci. (2017), DOI: 10.1007/s10853-017-1062-1

[21] A. Jedrzejewska, D. Sibera, U. Narkiewicz, R. Pełech, R. Jedrzejewski, Acta Phys. Pol. (2017), DOI: 10.12693/APhysPolA.131.1424

[22] E. K. Heidari, A. Ataie , M. H. Sohi, J.-K. Kim, J. Magn. Magn. Mater. (2015), DOI: 10.1016/j.jmmm.2014.12.014

[23] A. Rafferty, T. Prescott, D. Brabazon, Ceram. Int. (2008), DOI: 10.1016/j.ceramint.2006.07.012

[24] A.C.F.M. Costa, L. Gama, M.R. Morelli, R.H.G.A. Kiminami, Mater. Sci. Forum (2005), DOI: 10.4028/www.scientific.net/MSF.498-499.618

[25] S. Brunauer, P.H. Emmett, E. Teller, J. Am. Chem. Soc. (1938), DOI: 10.1021/ja01269a023

[26] L.L. Tian, Q.C. Zhuang, J. Li, C. Wu, Y.L. Shi, S.G. Sun, Electrochim. Acta (2012), DOI: 10.1016/j.electacta.2012.01.034

[27] D.A. Dikin, S. Stankovich, E.J. Zimney, R.D. Piner, G.H.B. Dommett, G. Evmenenko, S.T. Nguyen, R.S. Ruoff, Nature (2007), DOI: 10.1038/nature06016

[28] M.E. Uddin, T. Kuila, G.C. Nayak, N.H. Kim, B.C. Ku, J.H. Lee, J. Alloy. Compd. (2013), DOI: 10.1016/j.jallcom.2013.01.127

[29] B. Qiu, Y. Deng, M. Du, M. Xing, J. Zhang, Sci. Rep. (2016), DOI: 10.1038/srep29099

[30] B. Rajagopalan, J.S. Chung, Nanoscale Res. Lett. 9 (2014) 535. DOI: 10.1186/1556-276X-9-535

[31] Z. Wang, X. Zhang, Y. Li, Z. Liu, Z. Hao, J. Mater. Chem. A (2013), DOI: 10.1039/C3TA10433H

[32] Y. Yao, Z. Yang, D. Zhang, W. Peng, H. Sun, S. Wang, Ind. Eng. Chem. Res. (2012), DOI: 10.1021/ie300271p

[33] E. Yilmaz, T. Gürkaynak ,H. Deligöz, D. Deger, K. Ulutas, S. Yakut Proceedings of the 15th, IEEE International Conference on Nanotechnology, (2015), DOI: 10.1109/NANO.2015.7388975

[34] N. Ponpandian, P. Balaya, A. Narayanasamy, J. Phys.: Condens. Matter (2002), DOI: 10.1088/0953-8984/14/12/311